Ma 10: Auger- and Electron Energy Loss Spectroscopy

Tutor: L. Bogner

Benjamin Huber, Carolin Wille

October 23, 2011

Contents

1 Introduction

Auger electron spectroscopy (AES) and electron energy loss (EEL) spectroscopy are techniques, which are surface sensitive due to the small penetration depth of the electrons. Therefore, these methods can be used to analyze the cleanliness of a surface or the emergence of surface layers through adsorption. Furthermore, the spectra of AES and EEL allow to acquire information about fundamental processes within atoms and solid states, such as Auger transitions and plasmon excitations.

In this experiment an aluminum substrate will be analyzed by AES to detect impurities mainly due to oxygen adsorption. The probe will be cleaned by filing and the Auger spectrum of pure aluminum will be measured. The electron energy loss (eel) method will be used to detect the excitation of surface and bulk plasmons.

1.1 Electron Mean Free Path

As the mean free path of electrons depends characteristically on the energy of the electrons for a broad range of different materials, the so called universal curve (Fig. 1.1) is very useful in order to analyze the surface sensibility of spectroscopic methods. The minimal lies path exist between $40\,\mathrm{eV}$ and $100\,\mathrm{eV}$. Within this energy range the average penetration depth is below $10\,\mathrm{Å}$. Towards higher electron energies the mean free path increases only slowly and for $1\,\mathrm{keV}$ is still below $20\,\mathrm{Å}$. Therefore, any electron spectroscopic measurements within this energy range analyses surface properties rather than these of the bulk-solid.
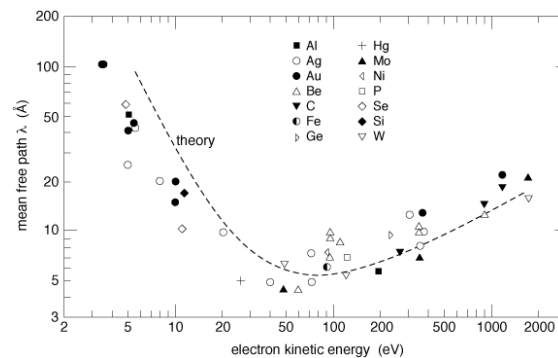
Figure 1.1: Mean free path of electrons in solids (logarithmic scale). Dots: Measurements. Dashed Line: Calculation. For Aluminium the mean-free path is even smaller then predicted by calculation. [**?**]

1.2 The Auger Process

If by any excitation an electron is emitted from the K level of an atom, an electron from a higher level transits to the level. Thereby an x-ray photon can emitted or the energy of the transition can be passed on to a third electron, which is thereby ionized. The latter process is called Auger process.

Nomenclature

The most commonly used nomenclature for the Auger electron spectroscopy is based on the quantum number n (K for $n = 1$, L for $n = 2$...), followed by an index to denote the different possible states for this n (in the order of increasing energy). To fully describe the Auger electron, all three participating states have to be mentioned in this way.

Alternatively it is possible to simply note the electron configuration at the end of the auger process. In this way $2s^0 2p^6$ corresponds to KL_1L_1 and so on.

Energy of Auger-Electrons

The energy balance of the Auger-transition reads

$$E(KLL') = E(K) - E(L) - E^*(L') , \tag{1.1}$$

where $E(KLL')$ is the energy of the Auger electron stemming from a transition KLL', E(K)/E(L) are the binding energies of the electrons in K/L-level and $E^*(L')$ is the binding energy of the electron in the L' state, where the asterisk denotes, that this energy is altered through the absence of the K and L electron towards.

$$E^*(L') = E(L') + C(LL', T) - R , \tag{1.2}$$

where $C(LL', T)$ stems from the coupling of the two holes in LL', T represents the final state and R is the relaxation energy arising from the reduction of repelling electronic force.

These formulas hold for free atoms. For an electron, that is emitted from the valence band of a solid the work-function, which gives the minimum energy needed to remove an electron from a solid to the solid surface, has to be taken into account.

Expected Transitions

For aluminum the ionization energy of the K-level is about $1.6\,\text{keV}$. Therefore, the typical energy of exciting electrons up to $3\,\text{keV}$ is sufficient to excite the Auger KLL-transitions, which are the transitions of highest energy. These have an energy range from approximately $1.3\,\text{keV}$ to $1.4\,\text{keV}$ and are listed in table 1.1. The LMM transition is also possible and its energy is around $70\,\text{eV}$ with again a multiplet splitting.

Auger line		Theoretical Energy (eV)
$KL_{2,3}L_{2,3}$	(^3P)	$(1398.1)^\alpha$
$KL_{2,3}L_{2,3}$	(^1D)	1393.5
$KL_{2,3}L_{2,3}$	(^1S)	1386.6
$KL_1L_{2,3}$	(^3P)	1358.5
$KL_1L_{2,3}$	(^1P)	1342.3
KL_1L_1	(^1S)	1304.0

Table 1.1: Theoretical energies [?] of KLL Auger-Transitions for Aluminum. $^\alpha$: Forbidden due to parity conservation.

1.3 Plasmons

The pseudo particle of fermi-gas oscillation is called a plasmon. These plasmons have characteristic energies, depending on the conduction electron density n.

$$E_p = \hbar \underbrace{\sqrt{\frac{ne^2}{m_e\epsilon_0}}}_{\omega_p}$$

A calculation for aluminum, which has a conducting electron density of $n = 1.8 \times 10^{29} \mathrm{m}^{-3}$ yields $E_p(Al) = 15.8$eV. Apart from the more obvious bulk plasmons (three dimensional oscillations in the sample) there are also surface plasmons when a material with positive dielectric constant (vacuum) interface with a material of negative dielectric constant (Al). Literature values [?] for the bulk and surface plasmons of aluminum are 15.3eV and 10.8eV respectively.

An electron that excites a plasmon looses one of these characteristic energies and is said to have suffered plasmon loss. It is possible, that one electron suffers plasmon loss several times, leading to a series of equally spaced losses with decreasing intensity.

2 Experiment

The experiment is conducted within a vacuum chamber. Unfortunately, the evacuation during the experiment was not at the recommended value of about 10^{-10}mbar, but was constantly at about $4.3 \cdot 10^{-8}$mbar.

The excitation of the primary ionized electron was performed by high energetic electrons emitted from an electron gun placed within the vacuum chamber. The most central component of the experimental set-up is the cylindrical mirror analyzer explained below.

Concerning the experimental data, another important feature is the operating principle of the lock-in amplifier, which is used to process the signal from the detector. This analogue signal is then converted to a digital signal and is evaluated by a computer using an application of the software Labview.

2.1 Cylindrical Mirror Analyzer (CMA)

The CMA is an apparatus, which selects electrons within a small range of energy ΔE around a certain energy value E_0 from an electron source of various energies. This is performed by two cylinders, where the inner cylinder of radius r_1 has two ring-slits for the exit and entrance of the electron beam and a negative potential V is applied to the outer cylinder with radius r_2 (Fig. 2.1).
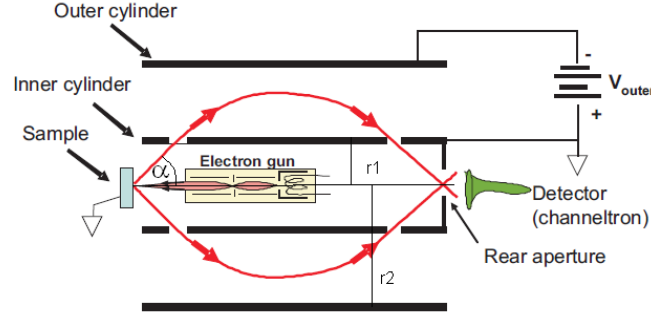
Figure 2.1: Schematic cross section of a CMA. [**?**]

Therefore, the electrons are bend towards the inner cylinder again. There exist a special emission angle $\alpha = 42°18,5'$, where the focusing properties are eminently better (focus of 2nd order). For CMAs operated at this angle the selected energy value is given by

$$E_0 = \frac{1.3099e}{\log r_2/r_1} V \ ,$$

(2.1)

where e is the electron charge. The energy resolution is determined by the angular spread of the emission angle $\Delta \alpha$ (Fig. 2.1) and given by

$$\frac{\Delta E}{E_0} = 2.75 \Delta \alpha^3 \ .$$

(2.2)

The current at the detector I is proportional to the number of incoming electrons $N(E)$. By measuring the voltage V, the function $N(E)$ is directly given by (2.1). However, the characteristic Auger-peaks are easier to detect considering the derivative $\frac{dN(E)}{dE}$. This can be achieved by a small sinusoidal modulation of the voltage with amplitude V_ω. The current I can then be expanded in terms of the small perturbation $V_\omega \sin \omega t$ as

$$I = I(V_0) + \frac{dI}{dV} V_\omega \sin \omega t + \dots \ ,$$

(2.3)

where the derivative $\frac{dI}{dV}$ represents the amplitude of the oscillating signal and is proportional to $\frac{dN(E)}{dE}$

$$\frac{dI}{dV} = A_\omega \propto \frac{dN(E)}{dE} \ .$$

(2.4)

This amplitude can be selected and amplified using a lock-in amplifier.

2.2 Lock-in Amplifier

In general the term lock-in amplifier refers to an amplifier, which is operated using an external characteristic signal, that is multiplied with the signal to be amplified, instead of an unspecific amplification. This characteristic external signal is related to the incoming signal, mostly via the frequency. E.g. during a measurement process a signal S_I of known frequency ω is created according to

$$S_I = A_0 + A_\omega \sin \omega t \ . \tag{2.5}$$

Then an amplification signal S_A of the same phase and frequency is used to amplify the incoming signal and afterwards an integration over a complete period is performed. The out-coming signal S_O is then proportional to the amplitude A_ω of the incoming signal S_I

$$S_O \propto A_\omega \ . \tag{2.6}$$

Therefore, the signal-to-noise relation can be significantly improved, as the constant off-set A_0 is almost completely eliminated form the signal.

3 Analysis

3.1 Oxidization

Due to the imperfect vacuum in the experimentation chamber, the Al is exposed to oxygen all the time. At the beginning of the measurements this shows as a significant buildup of oxygen atoms at the surface of the sample (see Figure 3.1a). Even though it can be removed very easily mechanically (Fig 3.1b), the constant presence of oxygen causes new oxidation. In the time of about 2 hours at $4.4 \cdot 10^{-8}$torr ≈ 317L the contamination had already reached more than 50% of the equilibrium level (Fig3.1c).
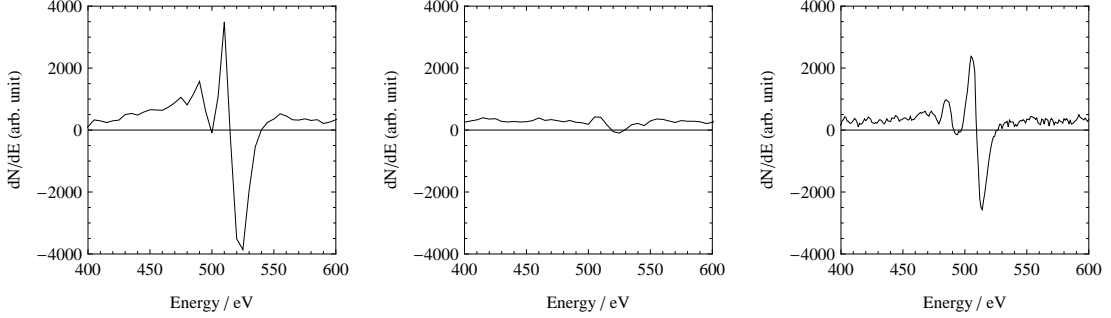
Figure 3.1: Differential detection rate at the oxygen specific energies before cleaning **(a)**, after cleaning **(b)** and after the experiments **(c)**. The characteristic minima are at approximately (477.8 ± 1.0)eV, (494.07 ± 0.30)eV and (514.12 ± 0.66)eV. Values obtained through the fitting of quadratic functions near the minima.

3.2 Auger spectrum of Al

With the cleaned sample, the differential spectrum of aluminium has its most noteable activity near 1400eV. The qualitative form of this region (Fig 3.2) is in very well agreement with the literature (cf. [?]) but quantitavely all values seem to be shifted towards higher energies.

This shift is expected, considering the poor alignment of the sample. A deviation from the perfect position Δx will cause a streching of the form

$$E' = \lambda(\Delta x) \cdot E, \tag{3.1}$$

where E' is the measured and E the actual energy of the electrons (cf. [?]). Assuming the deviation does not change significantly over the time of measurement, we can try to recalibrate our measurements with all three known minima in the oxygen spectrum. By comparison of the measured and the expected (cf. [?]) minima a stretching factor of $\lambda = 0.9918 \pm 0.0027$ can be calculated.

The values that have been corrected with this factor are consistent with the literature, but have a large margin of error due to the rather large relative error margin of the

literature values. Using the last minimum of the Al spectrum to calibrate the spectroscope in a similar way to $\lambda = 0.99527 \pm 0.00082$, results in better values. While this does not allow to compare the absolut values, the relative spacing between the minima can still be compared and confirmed. Due to the significant improvement in accuracy this last calibration will be used throughout the rest of this work.

The integrated version of this spectrum shows peaks corresponding to KLL auger effects in aluminium. The resolution is far too bad to allow the identification of all five expected transitions, but with a reference spectrum from [**?**] it is possible to identify the 5 most significant peaks. See Table 3.2 for more details.
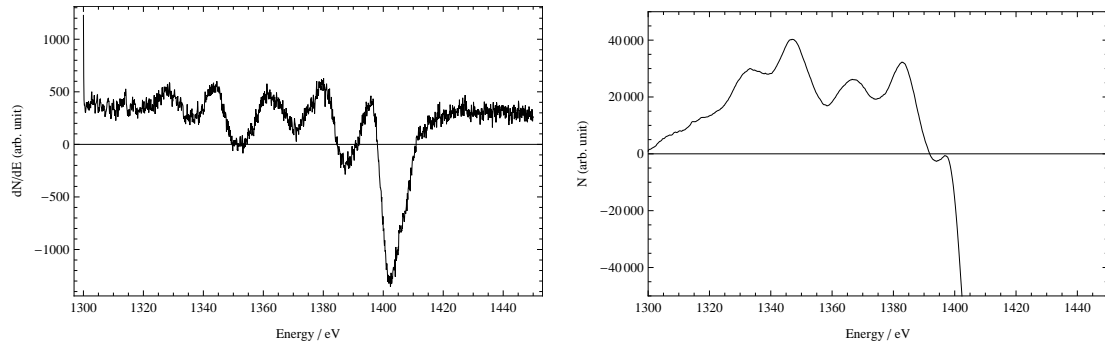
Figure 3.2: All values obtained by fitting quadractic functions near the minima (a) or maxima (b). **(a)** Measured differential detection rate of Al. Minima at (1336.07 ± 0.30)eV, (1352.52 ± 0.20)eV, (1370.73 ± 0.32)eV, (1388.32 ± 0.16)eV, (1402.64 ± 0.14)eV. **(b)** Integrated version of (a) after substracting an estimated noise level of 300. The peaks are at (1333.64 ± 0.64)eV, (1346.98 ± 0.03)eV, (1366.90 ± 0.05)eV, (1382.81 ± 0.04)eV, (1396.96 ± 0.08)eV.

O calibration	Al calibration	literature
(1325.1 ± 3.5)	(1329.7 ± 1.2)	1329
(1341.4 ± 3.5)	(1346.1 ± 1.2)	1345
(1359.4 ± 3.6)	(1364.2 ± 1.2)	1364
(1376.9 ± 3.6)	(1381.8 ± 1.2)	1380
(1391.1 ± 3.6)	(1396.0 ± 1.2)	1396

Table 3.1: Positions of the minima in the differential (dN/dE) aluminium auger spectrum. Values corrected with the information of the oxygen minima or the last aluminium minimum compared to the values in the literature [**?**]. All values in eV.

3.3 Plasmons

The most significant peaks in section 3.2 already contained electrons that suffered plasmon loss. These characteristic losses can be measured with electron energy loss spectroscopy. A measurement with higher energy electrons (1keV) shows mainly the bulk plasmons,

while a second measurement with weaker electrons (170eV) promises to show surface plasmons more clearly, due to the lower penetration depth.

In the measurements (see Fig 3.3), the most prominent peak is the on of the backscattered electrons. All preceding ones have suffered an increasing amount of plasmon loss and are thus expected at the energies $E = E_{\text{backscatter}} - B_n$, where B_n is the energy of the n-th harmonic of the bulk plasmon. In the approximation of an harmonic oscillator we can write $B_n = nB_1$ and can thus use all measured peaks to increase the accuracy of our first harmonics energy.

The first measurement (see Fig 3.3 right) resulted in a (weighted) mean energy for the bulk plasmons of $B_1 = (15.31 \pm 0.54)$eV. This result is consistent with the two bulk plasmons found in the 170eV measurement (see Fig 3.3 left). The single peak in the second measurement corresponding to a surface plasmon results in $S_1 = (11.04 \pm 0.20)$eV.

Both energies are identical to the result of Massignon et al [?] as well as the previously calculated value for the bulk plasmon (cf. 1.3).
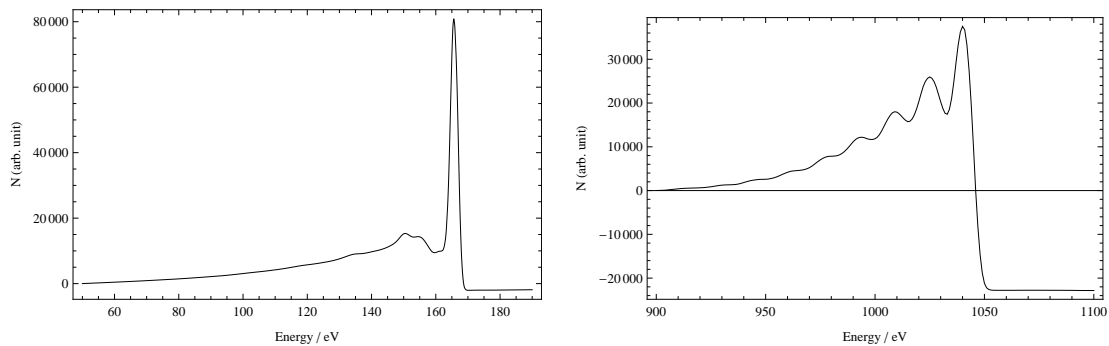
Figure 3.3: Electron backscatter spectra of Al including additional peaks due to plasmon loss. All values obtained by fitting quadractic functions near the maxima. **(a)** Measurement with electrons of about 170eV. Peaks at (135.84±0.09)eV, (150.52±0.03)eV, (154.55±0.05)eV, (165.65 ± 0.04)eV. **(b)** Measurement with electrons of about 1050eV. Peaks at (919.6 ± 6.7)eV, (934.5 ± 5.4)eV, (948.8 ± 1.7)eV, (964.7 ± 1.9)eV, (980.1 ± 1.2)eV, (994.11 ± 0.59)eV, (1009.31 ± 0.26)eV, (1024.96 ± 0.09)eV, (1039.90 ± 0.28)eV.

3.4 KLL Transitions within the Auger spectrum of Al

As the energies of the bulk and surface plasmons are now determined, a proper analysis of the Auger KLL spectrum can be performed. The plasmon losses are taken into account in order to match the peaks correctly and distinguishing pure Auger electrons from those electrons, that suffered plasmon loss. However, due to the very limited resolution of the used apparatus, it occurs that, whenever two significant peaks are closer than 7eV they merge, resulting in a single peak of the mean value. Therefore, not all transitions can be identified accurately (see table 3.2).

transition	literature	theory	measurement
$^1P + B_1$	1326.1	1327.4	(1327.3 ± 1.1)
^1P	1341.4	1342.3	(1340.6 ± 1.1)
^3P	1357.2	1358.5	(1360.4 ± 1.2)
$^1D + B_2$	1362.6	1361.9	
$^1D + B_1$	1377.9	1377.7	(1376.3 ± 1.2)
^1D	1393.2	1393.5	(1390.4 ± 1.2)
^1S	1387.2	1386.6	

transition	$^1P + B_1$	^1P	^3P	$^1D + B_2$	$^1D + B_1$	^1D	^1S
literature	1326.1	1341.4	1357.2	1362.6	1377.9	1393.2	1387.2
theory	1327.4	1342.3	1358.5	1361.9	1377.7	1393.5	1386.6
measurement	(1327.3 ± 1.1)	(1340.6 ± 1.1)	(1360.4 ± 1.2)		(1376.3 ± 1.2)	(1390.4 ± 1.2)	

Table 3.2: Characteristic (corrected) energies of the KLL auger spectrum of aluminium, their according transition and the literature and theory values from [**?**]. $+B_{1/2}$ denotes the change in energy due to the interaction with bulk plasmons.

4 Summary and Discussion

An aluminium sample was analyzed in a high vacuum chamber with both AES and EELS. The differential Auger electron spectrum was in good agreement with the literature. As the positional offset of the sample was unknown though, it was necessary to recalibrate the spectroscope using one of the measured peaks itself.

Due to the limited resolution of the used apparatus, the KLL spectrum of Aluminium could not fully be observed. The five peaks that were measurable though agree very well with the literature (see section 3.2).

The EELS to measure the energies of plasmons was a full success. Both the energy of the bulk plasmon $(B_1 = (15.3 \pm 0.6)\text{eV})$ as well as the energy of the surface plasmon $(S_1 = (11.0 \pm 0.2)\text{eV})$ agree with the theory, even though only one surface plasmon was observable.

Despite the good accuracy for the EELS measurements the accuracy for the AES was mediocre at best. While the instruments are precise enough (having negligible error margins compared to the total error), the experimental setup itself causes a lot of noise and is thus the main reason for the (high) errors in the performed experiments. A good place to start improving upon the setup probably is the vacuum pump as well as the positioning of the sample.